Showcasing research from a group of researchers led by Dr Shan Jiang and Dr Huiyu Liu, School of Physical Science and Technology, ShanghaiTech University, China.

Ferroelectricity in organic materials: from materials characteristics to *de novo* design

This perspective summarises synthetic strategies and design principles for accelerating the development of high-performance organic ferroelectrics. We show how empirical design principles, computational methods, and integration of computation and automation approaches can be used for designing new organic ferroelectrics. Further, we highlight some of the challenges that lie ahead and provide our views on possible solutions. Artwork was designed by Julie Liu from ShanghaiTech University.

As featured in:

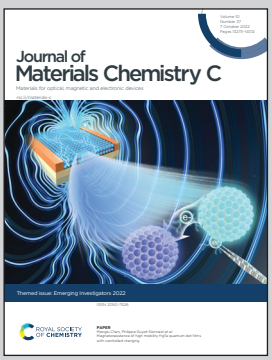

See Huiyu Liu, Shan Jiang *et al.*, *J. Mater. Chem. C*, 2022, **10**, 13676.

ROYAL SOCIETY OF CHEMISTRY

rsc.li/materials-c

Registered charity number: 207890

Journal of Materials Chemistry C

ROYAL SOCIETY OF CHEMISTRY

PERSPECTIVE

View Article Online
View Journal | View Issue

Check for updates

Cite this: J. Mater. Chem. C, 2022, 10, 13676

Ferroelectricity in organic materials: from materials characteristics to *de novo* design

Huiyu Liu, *[a] Yangzhi Ye,[a] Xiangyu Zhang,[a] Tieying Yang,[b] Wen Wen[b] and Shan Jiang *[a]

Received 1st April 2022,
Accepted 5th June 2022

DOI: 10.1039/d2tc01330d

rsc.li/materials-c

Supramolecular chemistry exploits weak, reversible interactions to form complex structures from simple components, which offers a solution for designing new ferroelectric materials. Organic ferroelectrics have been considered to be promising alternatives to conventional inorganic ferroelectrics due to their molecular mobility, flexibility and tunability of well-defined structures. However, ferroelectricity in organic solids remains underexplored, and the limited number of organic ferroelectrics with high performance hinders their practical applications. Therefore, the design of new organic ferroelectrics with promising ferroelectric properties is of great interest. In this perspective, we describe key material features and properties of organic ferroelectrics. Synthetic strategies and design principles are comprehensively reviewed. To further explore the possibility of organic ferroelectrics, we give our perspectives on the computational design and how to integrate computation and automation approaches for the accelerated discovery of organic ferroelectrics. Some of the challenges and opportunities in the field have been discussed. We hope this outlook can enable more research to accelerate the development of high-performance organic ferroelectrics.

Published on 08 2022. Downloaded on 23/07/2024 8:47:18 .

Introduction

A ferroelectric is a crystalline material whose spontaneous polarisation can be reversed in response to an external electric field below a certain temperature (the Curie temperature, T_c).[1] The switchable property of the polarisations enables ferroelectrics

[a] School of Physical Science and Technology, ShanghaiTech University, Shanghai 201210, China. E-mail: Jiangshan@shanghaitech.edu.cn, liuhy9@shanghaitech.edu.cn
[b] Shanghai Advanced Research Institute, Chinese Academy of Sciences, Shanghai 201204, China

Huiyu Liu

Huiyu Liu: Huiyu completed her PhD at Durham University, UK, in 2020. She worked with Prof. John Evans and Prof. Ivana Evans on structural characterisations of ferroelectric materials using a Powder X-ray Diffraction (PXRD) technique. She has significant expertise and a proven publication track record in developing PXRD analytical methods for understanding phase transitions in molecular ferroelectrics. In 2021, she started her postdoc at ShanghaiTech University, China. Her ongoing research at ShanghaiTech University is developing new organic molecular ferroelectrics using AI-driven methods and high-throughput characterisation tools for the purpose of establishing a clear structure-property relationship of organic ferroelectrics.

Shan Jiang

Shan Jiang: Shan completed her PhD at the University of Liverpool, UK, in 2013 and she has worked with Prof. Andy Cooper (FRS) on the rational design of porous organic cages. After that, she worked at the University of Liverpool and Durham University for her postdoctoral studies. In 2019, she joined ShanghaiTech University as a PI, and her research interests include combining high-throughput computational and synthetic approaches to expedite new materials discovery, and designing new porous molecular materials with new functions, such as organic ferroelectrics.

This journal is © The Royal Society of Chemistry 2022

Published on 08 2022. Downloaded on 23/07/2024 8:47:18 .

to become a valuable material with a wide range of applications in electronic and optical devices, including random access memories, actuators, transducers, piezoelectric elements, and frequency multipliers.[2–6]

Most of the ferroelectrics used in electronic and optical devices are oxide-based ceramics that typically contain toxic metals and require high processing temperatures.[7] Organic ferroelectrics, on the other hand, have demonstrated desirable features and are considered promising alternatives to conventional inorganic ferroelectrics. A distinguishing feature of solution processability allows organic ferroelectrics to be cast into films or devices in an easy and efficient way, which offers a low-cost and environmentally friendly fabrication process.[1,8] However, ferroelectricity in organic solids remains underexplored to date. Few cases can be found applying organic ferroelectrics. Therefore, the discovery of new organic materials with promising ferroelectric properties near room temperature is of significant interest. Organic chemistry, especially supramolecular chemistry has provided effective strategies for designing high-performance ferroelectrics in a solid state.[8] The ferroelectricity in these materials arises from either the dynamic motions of molecules or the collective site-to-site transfer of electrons or protons between molecules.[9] This means the bistable polarisation can result from either intrinsic molecular dipoles or extrinsic diploes induced by non-covalent interactions between molecules such as hydrogen-bonding and charge-transfer interactions. The arrangement of organic molecules in a solid state has a significant impact on the physical properties of the materials. Thus, achieving ferroelectricity requires engineering the self-assembly of molecules, which in turn controls the inter and intramolecular interactions and motions.

For a material to be a good ferroelectric with usable properties, it must have a high spontaneous polarisation (P_s), high saturation polarisation (P_{sat}), high dielectric constant (ε_r), low dielectric loss, and a T_c near or even above room temperature. Material performance optimisation has long been an important topic for the development of organic ferroelectrics. Polyvinylidene difluoride (PVDF)-based ferroelectric polymers have been known for several decades, and they have exhibited excellent ferroelectric and piezoelectric properties.[10] Very recently, a ferroelectric polymer have shown an exceptionally high electromechanical coupling at a low electric field.[11] However, the number of ferroelectrics in low-molecular weight organic compounds is rare. As shown in Fig. 1, by taking the advantages of supramolecular chemistry, some low-molecular-weight organic ferroelectrics with improved ferroelectric performance have been reported.[12–18] Even engineering a weak intermolecular interaction such as halogen bonding could strongly influence the property of a ferroelectric material.[19]

This perspective mainly focuses on the pure organic supramolecular systems, including single-component, two-component and supramolecular host–guest crystal systems and organic salts. We will give an overview of the fundamentals of ferroelectricity and provide a comprehensive review of the chemical structure modifications of supramolecular ferroelectrics to improve their ferroelectric performances. Following that, we will discuss useful strategies and modular design approaches for discovering organic ferroelectrics. In order to obtain organic ferroelectrics with better performances, it is highly needed to exploit new organic molecules and establish the design strategy for material discovery. We will give our perspectives on the design principles, the computational methods, and how to integrate computation and automation approaches to accelerate the discovery of organic ferroelectrics.

1. Fundamentals of ferroelectricity

1.1 Ferroelectricity

Ferroelectrics are characterised by the switching property of spontaneous polarisations under an external electric field. A crystalline solid must adopt a polar space group to be ferroelectric. Ten polar point groups exist which are 1, 2, *m*, *mm*2, 4, 4*mm*, 6 6*mm*, 3 and 3*m*.[20] To be a ferroelectric, a material has to exhibit a permanent spontaneously generated electric polarisation while the orientation of its electric polarisation can be reversed in response to an applied electric field[21,22] as demonstrated by the polarisation–electric field (*P*–*E*) hysteresis loop in Fig. 2(a). When a ferroelectric crystal is under a positive electric field in a certain direction, the dipoles are gradually directed in the same orientation as the external electric field leading to a

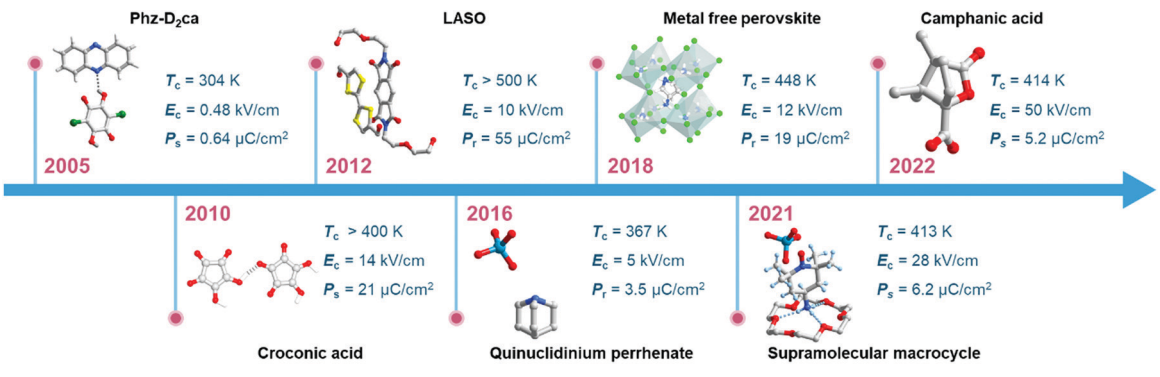

Fig. 1 Historical timeline for the development of organic ferroelectrics.[12–18]

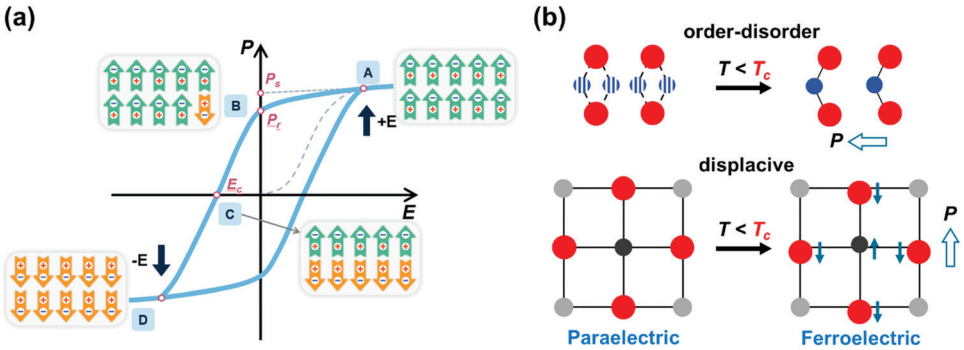

Fig. 2 Schematic representations of ferroelectricity. (a) Schematic diagram of the hysteresis loop of polarisation (*P*) *versus* electric field (*E*). The values of P_r, P_s, and E_c are derived from the *P*–*E* loop. (b) Schematic diagram of order–disorder type and displacive type phase transition.

Published on 08 2022. Downloaded on 23/07/2024 8:47:18 .

macroscopic saturation polarisation, denoted as P_s (position A in Fig. 2(a)). When the electric field is removed (position B), the majority of dipoles remain parallel to each other, giving rise to a remanent polarisation P_r. Once applying a negative electric field at this stage, the dipoles are gradually reorientated to the point (position C) where there is an equal number of oppositely directed dipoles. The electric field which results in zero net polarisation is called the coercive field E_c. When the maximum negative saturation polarisation is reached at position D corresponding to a negative saturation polarisation, $-P_s$, the dipoles are all aligned to the direction of the applied negative electric field. The area enclosed by the *P*–*E* hysteresis loop gives a measure of the energy required to achieve switching. This switchable property of the polarisation makes ferroelectrics useful in many technological applications.[2,3,23]

1.2 Phase transitions in the solid state

A ferroelectric material normally undergoes a structural phase transition from a paraelectric phase to a ferroelectric phase at the Curie temperature T_c. Above T_c, the paraelectric phase always adopts a non-polar point group, especially a centrosymmetric point group. As the temperature decreases, the molecular motion strength is weakened, which is associated with symmetry breaking during the phase transition. Below T_c, the ferroelectric phase adopts a polar point group which obtains a lower crystal symmetry.[24] The phase transitions in conventional organic ferroelectrics can be generally divided into two types: the order–disorder type and the displacive type as sketched in Fig. 2(b). The order–disorder type phase transition is frequently observed in organic ferroelectrics due to the large motional degree of freedom of organic molecules.[25] The driving force for the order–disorder type phase transition is the ordering of the molecular dipoles. In the high-temperature paraelectric phase, dipoles are disordered and thus cancel each other out. When the temperature decreases, the dipoles will rearrange in an ordered fashion leading to a polar structure at low temperatures. The displacive type phase transition occurring in the organic ferroelectrics is closely related to the dynamics of charges, ions and molecules.[26–29] The subtle change of an atomic or molecular position can give rise to symmetry breaking and thus a paraelectric-to-ferroelectric phase transition will take place. It needs to be noted that the order–disorder and displacive type phase transitions are not mutually exclusive.

1.3 Characterisation of ferroelectrics

The *P*–*E* hysteresis loop discussed above is a decisive analytical technique to validate ferroelectricity. However, due to the complicated nature of ferroelectricity, a wide range of characterisation methods are required to aid the *P*–*E* hysteresis loop.

Piezoresponse force microscopy (PFM). PFM is a scanning-probe microscopy-based technique, which can be used to perform polarisation dynamics and ferroelectric domain imaging and manipulation on the micro- or nanoscale.[30] PFM is based on the piezoelectric nature of ferroelectric materials that can produce strain under an external electric field. As shown in Fig. 3(a), PFM works by detecting subtle displacement of the samples in response to the electric field excitation. A conductive probe applied with V_{DC} and V_{AC} is in contact with the sample surface. The direction of polarisation can be determined by detecting an in-plane or out-of-plane piezoresponse to the voltage. The sample dimensions could change in either a vertical or a lateral direction, leading to the displacement of the tip cantilever. The amplitude and phase of both vertical and lateral signals of the tip displacement are detected by the laser irradiation on the probe and recorded on the photodetector, and are magnified separately by different Lock-in amplifiers.[31] A typical ferroelectric will show a butterfly-shaped curve in the amplitude *versus* voltage plot and a hysteresis loop in the phase *versus* voltage plot. The former can be used to identify the sample strain behaviour, while the latter is dependent on the switching behaviour of polarisation in a ferroelectric material. The contribution of the PFM technique to the design and discovery of high-performance ferroelectrics has been comprehensively reviewed.[32]

Second harmonic generation (SHG). SHG is a second-order nonlinear optical phenomenon, which only occurs in the non-centrosymmetric crystals, and the 10 polar point groups of ferroelectrics can have the SHG signal.[33] Since the paraelectric-to-ferroelectric phase transition is normally a symmetry lowering phase transition, the centre of the symmetry disappears in the ferroelectric phase. This means only material in its ferroelectric phase can exhibit an SHG signal. As shown in

 This journal is © The Royal Society of Chemistry 2022

Published on 08 2022. Downloaded on 23/07/2024 8:47:18 .

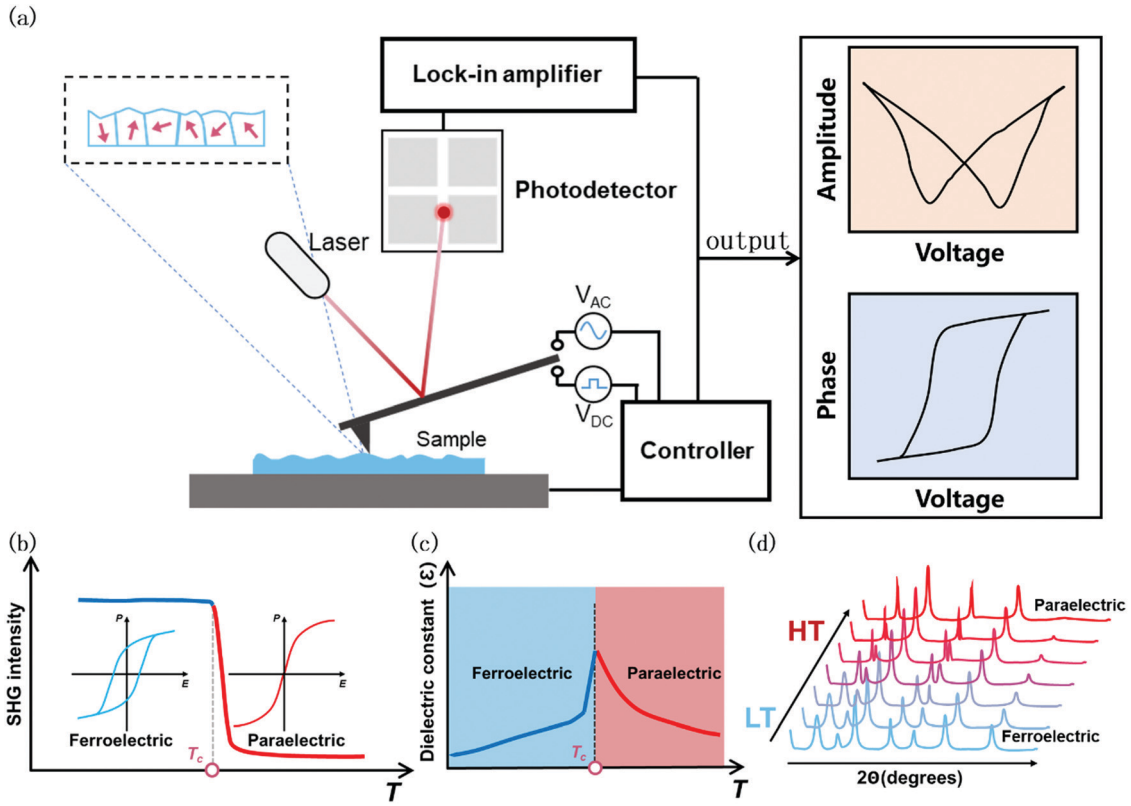

Fig. 3 Schematic diagram of the characterisation methods for ferroelectrics. (a) Sketch of the PFM working principle. (b) Schematic diagram of SHG measurement: during the phase transition, ferroelectrics lose the center of symmetry in the low-temperature ferroelectric phase, resulting in the appearance of the SHG signal. (c) Schematic diagram of dielectric measurement, the permittivity of ferroelectrics changes abruptly near the T_c. (d) Schematic diagram of VT-PXRD: when ferroelectrics undergo a phase transition, subtle changes in the crystal structure can be detected by PXRD. The decrease of crystal symmetry corresponds to the appearance of extra diffraction peaks.

Fig. 3(b), once the sample is heated above T_c, the SHG signal vanishes along with the phase transition, which enables variable temperature SHG measurement as a powerful characterisation method to demonstrate the structural phase transition.

Dielectric measurements. Dielectric property refers to the ability of a material to be polarised in an applied electric field. In general, polar materials with permanent polarisation have larger dielectric constants than non-polar materials. Dielectric measurements are commonly used to identify the phase transitions and T_c. As sketched in Fig. 3(c), when a ferroelectric material undergoes a phase transition, a peak anomaly in the dielectric content can be observed at T_c. On the basis of the Curie–Weiss law, the temperature dependence of the dielectric constant above T_c is often described by the following equation (ε_0 is the vacuum permittivity, and C is the Curie constant):[34,35]

$$\frac{\varepsilon}{\varepsilon_0} = \frac{C}{T - T_c}$$

Variable temperature X-ray diffraction (VT-XRD). XRD is a crucial analytical technique used to precisely determine the crystal structures and reveal the structural changes of material during phase transition. Single crystal XRD is a powerful tool to solve the structure at different temperatures. It can provide accurate information about atomic coordinates as well as bond lengths and angles. Powder X-ray diffraction (PXRD) is another efficient analytical technique to routinely analyse the structure of bulk samples. Since ferroelectricity is always accompanied by a structural phase transition, VT-PXRD is an effective method to investigate the structural changes of material. Once VT-PXRD is used to refine crystal structures, it can provide precise information on unit cell parameters and their temperature-dependent behaviours. As shown in Fig. 3(d), the paraelectric phase usually exists at high temperatures while the ferroelectric phase exists at low temperatures. During the paraelectric-to-ferroelectric phase transition, symmetry lowering normally occurs. It can be reflected in a PXRD pattern where extra reflection peaks appear below T_c. To gain detailed information on phase transition behaviours, high-quality and high-resolution PXRD patterns collected by using synchrotron radiation are normally required.

Symmetry-adapted distortion mode, commonly referred to as "distortion mode", has been developed for understanding the phase transition behaviors of a material by analyzing single crystal or powder diffraction data.[36] Distortion mode analysis is based on the group-subgroup relationship between crystal symmetry before and after the phase transition. As an effective analytical approach, distortion modes can help capture the subtle structural changes and describe the order parameters

Published on 08 2022. Downloaded on 23/07/2024 8:47:18 .

that break the symmetry by using a small number of parameters.[37] This method is widely employed to understand the phase transition behaviours for a variety of functional materials typically ferroelectric, ferromagnetic and ferroelastic materials.[38–42] As a result, we will be able to gain insights into the nature of a phase transition and build a structure-property relationship of a material.

2. Physical properties and applications of organic ferroelectrics

Due to the absence of the centre of symmetry, ferroelectrics intrinsically possess piezoelectric and pyroelectric properties for applications in optical and electrical fields such as energy harvesting, data storage and sensing. Other types of properties such as multiferroicity and photo-switchable ferroelectricity also entered the scene in the past few years. In this section, the physical properties and applications of organic ferroelectric materials are introduced.

2.1 Pyroelectric and piezoelectric properties

The relationship between ferroelectric, pyroelectric and piezoelectric materials refers to their point group symmetry. Ferroelectrics are a sub-class of pyroelectric and piezoelectric materials.[43,44] The piezoelectric effect is a phenomenon by which mechanical energy and electrical energy can be converted into each other. The material can generate a voltage under mechanical pressure, which is the direct piezoelectric effect.[43] On the contrary, the piezoelectric material can generate a mechanical strain under the application of an external electric field. This opposite process is called the converse piezoelectric effect. Many ferroelectrics are used in energy harvesting due to their excellent piezoelectric properties.[5,45,46] As a subgroup of piezoelectric materials, pyroelectrics need to crystallise in 10 polar point groups. In addition to being non-centrosymmetric, pyroelectrics have unique polar axes to generate spontaneous polarisation, and can produce polarity in the absence of an electric field. The pyroelectric effect refers to the accumulation of electric charges on the surface of a pyroelectric body as the ambient temperature changes uniformly, resulting in a potential difference. According to this characteristic, pyroelectrics have been widely used for sensing.[47]

2.2 Multiferroicity

Combining ferroelectricity with other ferroic properties such as ferromagnetism and ferroelasticity has drawn much attentions. The materials with two of the three ferroic order parameters coexisting are defined as multiferroics.[48] Great progress has been made in ferroelectrics that contain metal ions, however pure organic multiferroic materials are still rare.[49–51] Several excellent reviews comprehensively discussed the history and development of multiferroicity.[52,53] The discovery of magnetic ferroelectrics presents challenges because there is contraindication between ferromagnetism and ferroelectricity.[54] The diversity of materials, mechanisms and switching dynamics has been exploited to support multiferroicity. For example, the symmetry breaking in a charge-transfer ferroelectric can lead to polarisation switching.[55,56] Due to the redistribution of the electronic charge, the ferroelectrics have the potential to be magnetic as well.[57,58] Recently, homochiral organic ferroelectric (*R*)- and (*S*)-*N*-3,5-di-*tert*-butylsalicylidene-1-4-bromophenylethylamine (SA-Ph-Br(*R*) and SA-Ph-Br(*S*)) have been reported to show interesting photochromic behaviour.[59] In these materials, ferroelectricity and ferroelasticity coexist, and both can be controlled under photoirradiation. However, the design strategies limit the scope of possible accessible materials and leave a vast area of chemical space unexplored.

2.3 Photochromic property

Photochromic ferroelectrics have been shown great interest as stimuli-responsive functional materials.[60–70] Photochromism is the reversible transformation of a molecule between two isomers with different absorption spectra.[71] Photochromism involves chemical bond rearrangement leading to electronic and geometrical structure changes of molecules. Full optical control of ferroelectricity is a fascinating topic due to the potential interactions between light and ferroelectric order parameters. This may provide photoswitchable ferroelectrics with novel applications in data storage and sensing. Recently, single-component photochromic organic molecules have been reported to display ferroelectricity.[61–63] Particularly, the ferroelectric domains can be switched under UV light illumination by using a thin film sample of 3,4,5-trifluoro-*N*-(3,5-di-*tert*-butylsalicylidene)aniline (TFTBSA).[62] This means the polarisation switching can be achieved by optical control. Despite recent achievements in various photochromic ferroelectrics, quantitative conversion in the photochemical reaction in the solid state remains a significant challenge.

3. Synthetic strategies for enhancing ferroelectric performance

Emerging examples of organic ferroelectrics have shown potential applications. However, there are much fewer organic ferroelectrics exhibiting high performance. A number of challenges have existed. In this section, we introduce a wide range of synthetic approaches that have been employed to improve the phase transition temperatures and ferroelectric properties including P_s, P_{sat} and ε_r. The synthetic strategies mainly focusing on modulating the intermolecular interactions and controlling the molecular motions are discussed below in detail.

3.1 Elevating phase transition temperature (T_c)

One of the main obstacles that prevent organic ferroelectrics from practical applications is the low phase transition temperature compared to conventional inorganic ferroelectrics. Controlling the strength, geometry and dimensionality of intermolecular interactions is of great importance in enhancing the material performance of organic ferroelectrics.[72] For example, the highly directional hydrogen bonding is always closely

 This journal is © The Royal Society of Chemistry 2022

Published on 08 2022. Downloaded on 23/07/2024 8:47:18 .

related to ferroelectricity and its geometry has long been known to correlate with T_c.[73]

H/D substitution (deuteration) is a common method to increase the T_c of hydrogen-bonded organic ferroelectrics dramatically since the dynamics of hydrogen are crucial to the phase transition. The early example of hydrogen-bonded ferroelectric Phz-H2ca[12,74,75] undergoes a paraelectric-to-ferroelectric phase transition at T_c = 253 K. Its ferroelectricity is attributed to the movements of a proton between molecules. After H/D substitution, the deuterated Phz-D2ca undergoes a phase transition at T_c = 304 K. Deuteration not only elevated T_c by 51 K, but also proved the significant role of hydrogen bonding in ferroelectricity. In general, isotopes are different in atomic mass, volume, and spin, thus molecules can show distinctive supramolecular interactions due to the isotope effect.[76] It is well known that the replacement of H with D atoms can change the hydrogen-bond geometry, such as the elongation of proton donor–acceptor distance. This phenomenon is known as the Ubbelohde effect[77] and is the main reason why T_c can be raised in a hydrogen-bonded ferroelectric. Aside from the geometric change, deuteration can also lead to a mass-dependent effect. The localisation of the H (or D) atom in one of the potential minima is hampered by quantum tunnelling. The heavier D atom shows lower tunnelling frequency, and thus can result in a higher T_c. The large increase in the T_c could be the dual effect of both a geometric isotope effect and tunnelling frequency change.[78,79] Other substitution reactions such as $^{16}O/^{18}O$, Cl/Br and H/F substitutions were also reported to be effective strategies for constructing above-room-temperature ferroelectrics.[80–83] It is worth noticing that the effect of H/F substitution on T_c is applicable for a wider range of ferroelectrics including organic salts[84] and organic–inorganic perovskite-type[85] ferroelectrics, even though in these ferroelectric materials hydrogen-bonding interactions are not important for ferroelectricity.

Another useful strategy to elevate T_c is to confine the correlated motions of molecules or ions. An extreme case to exemplify this is a pure organic host–guest system. The $[MeO–C_6H_4–NH_3]^+$ cation can form supramolecular assembly with 18-crown-6 molecule *via* N–H···O hydrogen-bonding interactions, which acts as the counter cation of either $[BF_4]^-$ or $[TFSI]^-$ anions.[86,87] The ferroelectricity of both supramolecular macrocycle-based molecules originates from the reorientation of the guest cation $[MeO–C_6H_4–NH_3]^+$ driven by a pendulum-like motion. However, compared to $[BF_4]^-$ anions, the bulky $[TFSI]^-$ anion not only displays larger steric hindrance but also contains a proton acceptor to form hydrogen-bonding interactions with the cation *via* C–H···O–S bonds. As a result, the flip-flop motion of the cation was restricted, causing a significant increase in T_c by 288 K. The fine-tuning of supramolecular interactions and molecular motions can largely raise the T_c and enables room-temperature ferroelectricity in the supramolecular ferroelectric systems.[17,18,88,89]

3.2 Enhancing ferroelectric properties

It has long been an issue that organic ferroelectrics do not show good performance as inorganic ferroelectrics. Even though organic ferroelectrics have the potential to be used in portable devices due to their lightweight, solution-processibility and mechanical flexibility, high ferroelectric properties such as high P_s, high P_{sat} and high ε_r are still rarely observed in an organic ferroelectric, especially in their polycrystalline forms. Croconic acid[13] is a single-component ferroelectric which exemplifies how a molecular system can give rise to low-field and above-room-temperature ferroelectricity. It shows a high P_{sat} up to 30 μC cm^{-2} and its ferroelectricity can be robust to 400 K. The value of P_{sat} is even higher than some of the commercial inorganic ferroelectrics, such as $SrBi_2Ta_2O_9$[90] and $BaTiO_3$.[91]

In terms of practical applications, once the thickness of the ferroelectric thin film is down to the nanometre scale, it needs a coercive field on the scale of 100 kV cm^{-1} to achieve fatigue-resistant switching properties without significant current leakage.[92,93] However, organic ferroelectrics normally show a low coercive field since they need to overcome a relatively low energy barrier due to the weak interactions between molecules. Engineering the intermolecular interactions has been reported to be an effective strategy to largely increase the coercive field of an organic ferroelectric. The metal-free organic ferroelectric MDABCO–NH_4I_3 shows a high P_{sat} up to 22 μC cm^{-2} which is comparable to BTO (P_{sat} = 26 μC cm^{-2}).[16] However, this organic ferroelectric with excellent ferroelectricity properties still cannot meet the requirement for practical applications in flexible devices since the coercive field is far below 100 kV cm^{-1}. By replacing the I^- anion with PF_6^-, a new organic perovskite was synthesised where strong intermolecular interactions formed between the $MDABCO^+$ cation and the highly electronegative F in PF_6^- anion *via* N–H···F bond.[94] After introducing extensive intermolecular hydrogen bonds in the crystal structure, the coercive field of MDABCO–$NH_4(PF_6)_3$ finally reached 110 kV cm^{-1}, which is about an order of magnitude higher than MDABCO–NH_4I_3.

Another drawback of organic ferroelectrics is the uniaxial ferroelectricity, which often prevents the polycrystalline sample from observing the ferroelectric *P*–*E* hysteresis loop. Normally, the ferroelectricity of organic materials is investigated in its single-crystal form. This is due to the low symmetry of the crystal structures which could only give rise to uniaxial ferroelectricity. The random orientation of polycrystalline samples could almost cancel out the macroscopic ferroelectric response. Observing ferroelectricity in polycrystalline form requires the development of multiaxial ferroelectrics. The formation of plastic/ferroelectric materials offers the opportunity to design multiaxial ferroelectricity in organic substances.[15,84,89,95] It is commonly observed in supramolecular host–guest ferroelectrics where the dramatic flip-flop motion of the polar guest molecule gives rise to ferroelectricity.[96] Similar to the molecular rotator, molecular rotation was also observed in a family of closely packed organic salts. The globular cation $HDABCO^+$ was used to form a high-symmetric plastic crystal with different tetrahedral anions.[97] Such crystals normally crystallise in a cubic crystal system and show orientational disorder of the cation. The paraelectric-to-ferroelectric phase transition observed in these materials originates from the frozen cation rotation. Thus, the ferroelectric polarisation switching is

Published on 08 2022. Downloaded on 23/07/2024 8:47:18 .

attributed to the reorientation of the polar organic cation. Due to the high symmetry of the paraelectric phase, many of the plastic/ferroelectric show multiaxial ferroelectricity.[98,99] The ferroelectric *P–E* hysteresis loop can be measured unambiguously by using polycrystalline thin films or pressed pellets.[100]

4. Empirical design principles for the discovery of new organic ferroelectrics

There is an increasing drive to develop new organic ferroelectrics using empirical design principles to further enhance material performances. Ferroelectricity requires not only diploes aligned in an ordered manner without cancelling out each other, but also the source of the bistable polarisation. Some design principles based on polarisation switching mechanisms have been employed to synthesise new materials. Sachio and Yoshinori summarised design principles involving an acid-base combination and charge-transfer systems for cocrystals with promising ferroelectric properties in 2008.[1] Recently, Xiong and coauthors coined the term ferroelectrochemistry to describe the design principles for molecular-based ferroelectricity,[5] which includes quasi-spherical theory, H/F substitution and introducing homochirality. In this section, we will summarise four commonly used design principles for organic ferroelectrics, which are: (1) incorporating polar compounds that show orientational changes, (2) assembling hydrogen-bonded compounds that show intermolecular proton transfer through proton tautomerization, (3) assembling π–π stacking compounds that show intermolecular charge transfer and molecular displacements simultaneously and (4) design principle of bowl-to-bowl inversion, and recent advances by exploiting these strategies.

4.1 Design of molecular-reorientation type ferroelectrics

One of the conventional design principles for supramolecular ferroelectrics involves the use of freely rotating polar molecules. The disordering of the polar molecules triggers the phase transition above T_c, which refers to an order–disorder type phase transition.[101,102] Under the external electric field, due to the rotational degree of freedom, the orientation of molecular dipoles is reorganised when the direction of the electric field has switched (Fig. 4(a) and (b)). The key challenge of designing such organic ferroelectrics is to overcome the energy barrier for significant molecular reorientations in the solid state. In a closely packed crystal, molecular motions can be prevented by steric hindrance. Incorporating polar molecules into a supramolecular macrocycle or porous frameworks has been demonstrated to be able to promote the molecular motions and create excellent ferroelectricity, for example, supramolecular host–guest systems based on the crown ether[87,103] and encapsulation of a polar molecule such as ethanol within the pores of Metal Organic Frameworks (MOFs).[104]

Quasi-spherical theory (Fig. 4(c)) for controlling molecular rotation is of particular use for an order–disorder type organic ferroelectrics. Classic examples of organic ferroelectrics with high performance are metal-free perovskite ferroelectric[16] and organic salts[15,105,106] consisting of a polar $HDABCO^+$ cation or its derivatives. MDABCO–NH_4I_3 undergoes a paraelectric-to-ferroelectric phase transition at T_c = 448 K. The polar $MDABCO^+$ cations rotate freely in the high-temperature paraelectric phase and align in the same direction in the low-temperature ferroelectric phase. The hysteresis *P–E* loop measured from a single crystal can be obtained clearly up to 418 K which indicates promising practical applications in the devices.

4.2 Design of proton-transfer type ferroelectrics

The hydrogen bond can play a crucial role in inducing crystal polarity. Potassium dihydrogen phosphate (KDP) is a prototype ferroelectric in which the polarisation reversal originates from the proton transfer between two energetically equivalent sites on hydrogen bonds (Fig. 5(a)). The polarisation switching mechanism of KDP has inspired a number of organic ferroelectrics. To obtain KDP-type hydrogen-bonded organic ferroelectrics, two requirements were identified by Horiuchi and

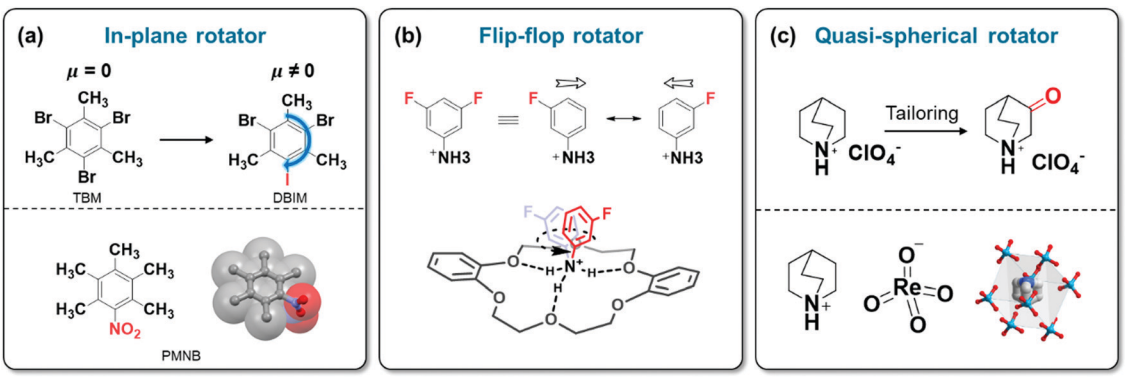

Fig. 4 Molecular-reorientation type ferroelectrics. (a) In-plane molecular rotators of DBIM, TBM(top)[101] and PMNB(down).[102] Reproduced from ref.102 with permission from the Royal Society of Chemistry. (b) Flip-flop dipole rotator of *m*-$FAni^+$ in *m*-$FAni^+$(DB[18]-crown-6)$[Ni(dmit)2]^-$ crystals. (c) Quasi-spherical rotator of [3-oxoquinuclidinium]ClO_4 after tailored(top),[105] and plastic ferroelectrics of [quinuclidine]ReO_4(down).[15] The crystal structure is generated using a structure (CCDC 1419397) from the Cambridge Structural Database.

 This journal is © The Royal Society of Chemistry 2022

Published on 08 2022. Downloaded on 23/07/2024 8:47:18 .

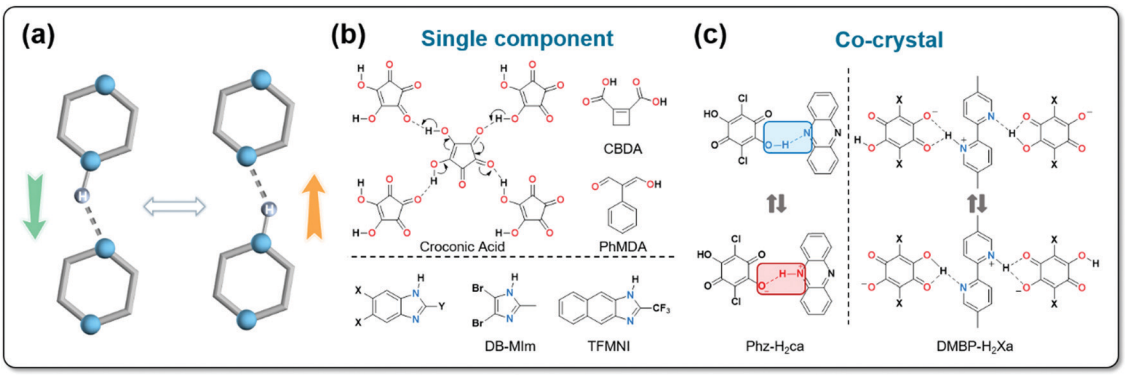

Fig. 5 Proton-transfer type ferroelectrics. (a) Schematic diagram of proton transfer in ferroelectric crystals. (b) Chemical structures of prototropic ferroelectrics: β-diketone enol(top)[119] and imidazole(down).[110] (c) Co-crystal of Phz-H_2ca[34] and DMBP-H_2Xa.[120]

Tokura.[8] The hydrogen-bonding interactions must be strong enough to allow the collective site-to-site transfer of protons. This normally corresponds to a moderate to strong intermolecular hydrogen bond.[107,108] Meanwhile, the molecules must remain chemically identical before and after polarisation reversal. As demonstrated in Fig. 5(b), croconic acid is the first successful example of KDP-type single-component organic ferroelectrics. The molecular structure of croconic acid contains a unique β-diketone enol unit, promoting an excellent polarisation switching performance through proton tautomerism between the keto and enol form.[13,109] Due to the existence of the β-diketone enol unit, the molecule can act in a dual role of proton donor and acceptor. A similar effect could be observed in benzimidazole and its derivatives, in which imine–enamine tautomerisation allows the proton transfer between molecules.[110]

An acid–base combination is another conventional strategy to produce organic ferroelectrics *via* intermolecular hydrogen bonds (Fig. 5(c)). Anilic acid always acts as an acid component in this type. It has comparable acid dissociation constants to those of carboxylic acids, indicating the relatively strong proton donating ability. This molecule is also able to yield strong intra- or intermolecular hydrogen-bonding interactions through keto-enol tautomerisation.[1] This interaction could be responsible for the bistable polarisation in organic ferroelectric materials. Chloranilic acid phenazine (CA-Phz)[12,75,111–116] is a well-known organic ferroelectric cocrystal. It undergoes a phase transition on cooling to 253 K, where its paraelectric phase (monoclinic $P2_1/n$) transforms to a ferroelectric phase (monoclinic $P2_1$). Hydrogen bonds play an important role in its phase transition, evidenced by the significant change in the Curie temperature of the deuterated compound.[12] The discovery of ferroelectricity in CA-Phz motivated the development of several chloranilic acid-based ferroelectric cocrystals.[116–118]

4.3 Design of charge-transfer type ferroelectrics

Charge-transfer (CT) ferroelectrics complexes belong to electronic ferroelectrics in which electronic charge ordering is responsible for the polarisation switching. A CT complex contains electron donor (D) and electron acceptor (A) species and typically contains a mixed stack of D and A. In the crystal structure, when the donor and acceptor are stacked face-to-face, the electron will transfer from the HOMO of the donor to the LUMO of the acceptor, as sketched in Fig. 6(a). As a

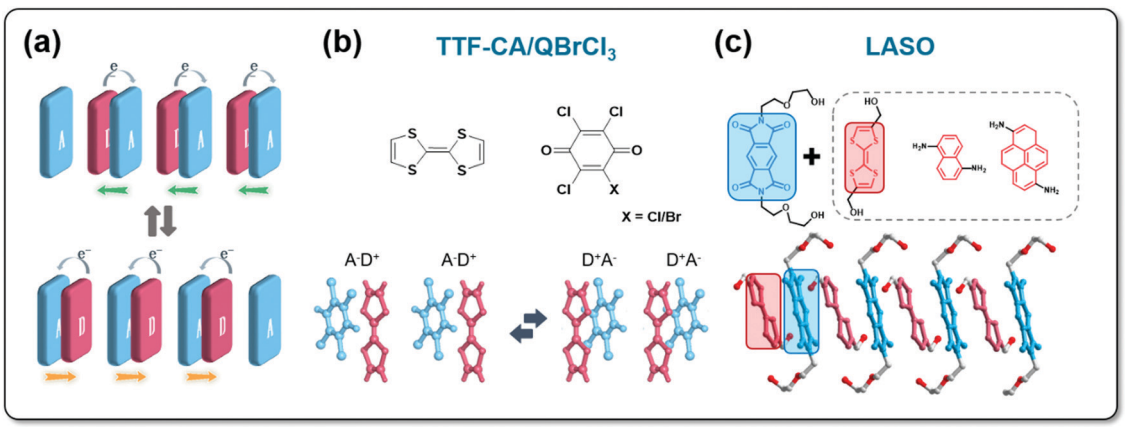

Fig. 6 Charge-transfer type ferroelectrics. (a) Schematic diagram of charge transfer in ferroelectric crystals. (b) Molecular structures of the TTF, CA, and $QBrCl_3$(top), polarisation reversal diagram of TTF-CA. Reproduced from ref. 56 with permission from the American Physical Society. (c) Chemical structure of electron donor (red) and acceptor (blue) molecules (top), and crystal structures of LASO complexes (down). The crystal structure is generated using structure (CCDC 981516) from the Cambridge Structural Database.

Published on 08 2022. Downloaded on 23/07/2024 8:47:18 .

consequence, the charge transfer occurs due to the valence instability. An inherent structural instability (also known as the Peierls instability) turns the equally spaced $D^+ A^- D^+ A^- D^+ A^-$ chain into the dimerised D^+A^-–D^+A^-–D^+A^- chain. The molecules in the crystal thus move relatively along the stacking axis, resulting in the crystal polarity. The polarisation reversal can be achieved by forming A^-D^+–A^-D^+–A^-D^+ chains. As shown in Fig. 6(b), tetrathiafulvalene-ρ-chloranil (TTF-QCl_4) and tetrathiafulvalene-ρ-bromanil (TTF-QBr_4) are the best-known examples of mixed-stack CT complexes.[121–124] Recently a supramolecular macrocycle consisting of quinones was used as an electron acceptor. Even though its ferroelectric behaviour is ambiguous, it may promote the development of new types of electron donors and acceptors.[125]

Lock-Arm Supramolecular Ordering (LASO)[14] is a newly developed strategy to allow CT complexes to co-crystallise rapidly into a polar structure. By following the LASO design (as shown in Fig. 6(c)), either an electron-donor or an -acceptor in a charge-transfer complex must be functionalised with ''long arms'' that can work as proton-donor and -acceptor for the formation of hydrogen bonds.[126] The assembly of molecules is stabilised simultaneously by charge-transfer, hydrogen-bonding, π–π stacking and van der Waals interactions. Due to the synergy of different interactions, the ferroelectric *P–E* hysteresis loop was successfully obtained at room temperature. The gigantic P_s is believed to result from both charge transfer and proton transfer.[127]

4.4 Design of bowl-to-bowl inversion type ferroelectrics

Bowl-to-bowl inversion is commonly capable of inducing ferroelectricity in liquid crystals.[128,129] The mechanism of polarisation switching is unique to any conventional approach. The reversal of polarisation is triggered by the up-and-down bowl-shaped structure inversion along the π-stacking direction. Recently, the organic molecules designed by the bowl-to-bowl inversion approach can form one-dimensional columnar stacking in solid crystalline form. As shown in Fig. 7, the trithiasumanene (SS) molecule with shallow bowl depth was selected as the bowl-shaped π-aromatic core.[130] The bowl-inversion barrier can be modulated by changing heteroatoms and side-chain length. During the phase transition of the CnSS (n = 6, 8, 10 and 16) molecules, in-plane molecular rotation and inversion take place at the same time. Above-room-temperature ferroelectricities of the CnSS series were validated by ferroelectric *P–E* hysteresis loops at 383, 363, 353 and 336 K, respectively.[131]

5. Perspectives on the computational methods for the discovery of organic ferroelectrics

Some progress has been made in the synthesis of new organic ferroelectrics with promising properties, however, it remains significantly challenging to intuitively predict or design ferroelectricity in organic systems. A comprehensive understanding of molecular assembly rules and structure–property relationships is needed to design new organic ferroelectrics.

5.1 Pseudosymmetry search

In crystals, ferroelectricity is observed only in materials adopting polar space groups. To find potential new molecular ferroelectrics, early studies searched polar crystal structures in the Cambridge Structure Database (CSD) and performed a pseudosymmetry study on the polar structures in order to predict high-symmetric paraelectric phase.[132–134] Some software has been developed for pseudosymmetry detection. Several new ferroelectrics have been reported by following these procedures. Zikmund *et al.* performed a symmetrical analysis on the polar crystal structures using the CSD, and found a weak ferroelectric, the cyclohexane-1,1′-diacetic acid in 1994.[135] Several single-component molecular ferroelectrics based on proton tautomerism were discovered using this method by Horiuchi *et al.*, especially the discovery of croconic acid in 2010.[13] All these compounds were extracted as the candidates from the CSD, and their ferroelectricity was confirmed by the *P–E* hysteresis loop. These materials also exhibited good material performances. However, searching for a polar crystal structure has not achieved much success because there are other factors

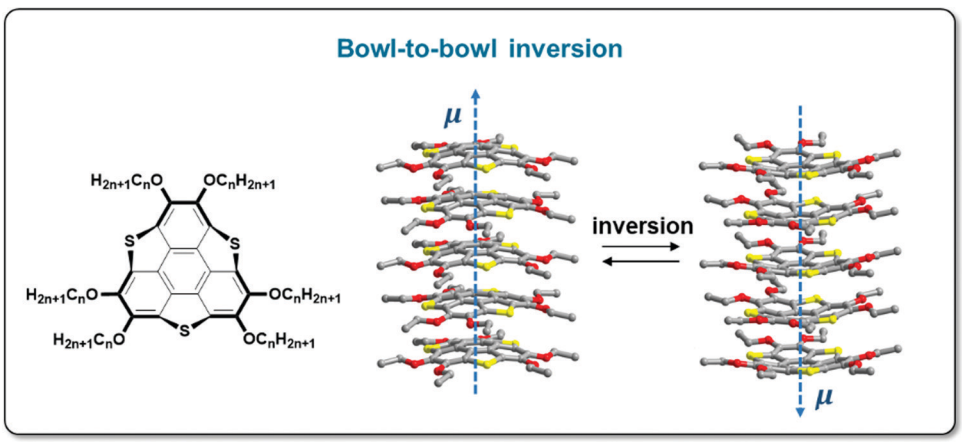

Fig. 7 Molecular structure and polarisation reversal diagram of CnSS. Reproduced from ref. 131 with permission from Springer Nature.

 This journal is © The Royal Society of Chemistry 2022

Published on 08 2022. Downloaded on 23/07/2024 8:47:18 .

needing consideration for ferroelectricity design. The relative interactions between adjacent dipoles can be cancelled out in the crystals, leading to antiferroelectricity. Therefore, organic ferroelectrics have been synthesised in large numbers but only a few ferroelectric properties have been found.

5.2 Computational simulations

The search for new organic ferroelectrics would involve ferroelectric mechanisms. This is a fundamental design challenge, relevant to all supramolecular materials, which can be addressed by simulations. Computational simulations can provide insights at all stages of the development and characterisation of supramolecular materials over a wide range of time and length scales from rationalising and predicting the structures and properties of organic ferroelectrics. A variety of computational methods have been applied to study different aspects of ferroelectrics. Theoretical spontaneous polarisation can be calculated by the Berry phase theory.[136,137] First-principles electronic structures calculations were performed to evaluate the spontaneous polarisation. For the hydrogen-bonded organic ferroelectrics, the calculated spontaneous polarisations are in good agreement with the experimental ones, which can be used to predict the material performance.[110] In addition, Stroppa and coauthors used molecular dynamic simulations to provide new insights into the mechanism of phase transition of di-isopropyl-ammonium halide molecular crystals.[138] Furthermore, Walsh and coauthors described the ferroelectricity of the proton transfer ferroelectric croconic acid by selecting the correct subset of its phonon modes and provided a deeper look at proton transfer ferroelectrics.[26] Kinetic Monte Carlo simulations were used to study switching kinetics in organic ferroelectrics. Both hysteresis loops and depolarisation curves were simulated for a large range of temperatures and timescales to investigate different flipping modes in this material.[139]

5.3 Crystal structure prediction (CSP)

The majority of the functional properties and the potential applications are related to their solid state. Therefore, elucidating the structure of the solid form and understanding how this is related to the observed behaviour of the material is a fundamental stepping stone in achieving the rational design of organic ferroelectrics. However, we believe there is a lack of research in the area. Zeng and coauthors applied Crystal structure prediction (CSP) and density functional theory (DFT) geometry optimisation to predict tens of thousands of packing structures and design new ferroelectric organic molecular crystals with ultrahigh polarisation.[140] Although the development of CSP methods was driven by the pharmaceutical industry, they have begun to be applied in the field of materials science in the last few years. Recently, CSP has been used to calculate the most energetically favourable crystal packing for porous organic cages (POCs). Energy structure-function (ESF) maps are a combination of CSP with each structure-property prediction, which is an exciting strategy for the screening of candidates of organic molecules for desirable properties.[141,142] By the fact that many thousands of polymorphs need to be screened for their crystal packings and accurately predicted solid state properties, CSP is currently computationally expensive. The ultimate goal is to identify more reliable methodologies (combined Machine learning (ML) approach with CSP) to predict molecular packing motifs and crystal structures and accelerate the discovery of new materials. We believe this would have a disruptive impact on the field of organic ferroelectrics.

5.4 High-throughput computation and synthesis

Additionally, to explore the vast possibility of supramolecular ferroelectrics and underpin the structure-function relationships, an efficient chemical toolkit would be of great utility. In the past few years, there has been emerging interest in the development of high-throughput computation and synthesis targeting the discovery of materials with particular applications.[143] For example, these methods have been successfully applied to many types of supramolecular materials such as POCs,[144] MOFs[145] and organic polymers.[146] However, the use of a high-throughput approach for supramolecular ferroelectricity is rare, which is partly due to the difficulties in predicting the structure and the difficulty raised in characterising the libraries of ferroelectrics. Given the vast organic material search space, we also believe integrating computational and robotic workflow might be a better platform to design and synthesise and evaluate extremely large numbers of materials. In this case, the number of materials that can be realised and tested will be increased by several orders of magnitude for accelerated organic ferroelectrics discovery. It can be expected that artificial intelligence (AI) algorithms can provide new ways to explore the chemical space of supramolecular ferroelectrics by truly performing the 'inverse design' of materials based on designing a material with optimal properties.

Summary and outlook

The field of ferroelectrics has just celebrated the centenary of the discovery of the Rochelle salt crystal.[147] However, taken as a percentage of all known organic molecules, ferroelectricity in organic solids remains underexplored, and the number of high-performance organic ferroelectrics is extremely rare, which hinders their practical applications. Therefore, the design of new organic ferroelectrics with promising ferroelectric properties should be of great interest.

In this perspective, we summarised several important aspects of organic ferroelectrics from the fundamentals of ferroelectricity to the chemical structure modification strategies for improving the ferroelectric performance of organic ferroelectrics. Design principles for new molecular ferroelectrics have been highlighted to accelerate organic ferroelectrics discovery.

Even though the field of organic ferroelectricity has reached some maturity after more than 100 years of research, many fundamental questions remain open, and the exploration of new systems is highly needed. We believe that the most

Published on 08 2022. Downloaded on 23/07/2024 8:47:18 .

important results and discoveries have not yet been realised. Here, we highlight some of the challenges and opportunities that lie ahead and can be tracked:

(1) The tendency to crystallise in a centrosymmetric structure makes organic molecules rarely possess ferroelectricity. How to construct polar crystal structure effectively is essential to creating ferroelectricity. The molecular crystal packing is often dictated by weak, competing intermolecular interactions which rarely obey simple rational design principles. Hence, the *a priori* design of materials with predetermined desirable properties is one of the most challenging tasks. The integration of CPS with property predictions to generate ESF maps would offer a strategy for autonomous design for polar crystal structures. For example, for hydrogen-bonded organic molecular ferroelectrics and charge-transfer organic molecular ferroelectrics, ESF maps could have a valuable role to play in the selection of building blocks and the virtual screening of candidates of organic molecules.

(2) Developing a polarisation switching process is key to ferroelectricity. How to overcome the energy barrier of the reorientation of dipole moments is crucial for achieving ferroelectricity in the solid state. Even though the diversity of design principles has vastly increased over the century, a few organic ferroelectrics are able to show high performance. Due to the close relationship between the crystal structure and the ferroelectricity, we would like to emphasise the fundamental importance of understanding the structure-property relationship for ferroelectrics design. The use of an XRD analytical method such as the symmetry-adapted distortion mode analysis and computational simulations would be a powerful combination for the comprehensive study of the structure-property relationship from both experimental and computational aspects.

In summary, we have given an outlook of the organic ferroelectric design principles. With these features in mind, we believe the research field will overcome a major bottleneck in the design and discovery process, offering the potential to accelerate material discovery.

Author contributions

S. J. and H. L. conceived the idea and led the project. All authors contributed to writing and revising the paper.

Conflicts of interest

There are no conflicts to declare.

Acknowledgements

This work was supported by ShanghaiTech University Startup Fund. S. J. also acknowledges financial support from the National Natural Science Foundation of China (22001169), the Science and Technology Commission of Shanghai Municipality (21JC1401700) and the Shanghai Pujiang Program. H. L. would like to acknowledge the support from the Shanghai Postdoctoral Excellence Program.

References

1 S. Horiuchi and Y. Tokura, *Nat. Mater.*, 2008, **7**, 357–366.
2 A. Kumar, S. Mukherjee and A. Roy, in *Ferroelectric Materials for Energy Harvesting and Storage*, ed. D. Maurya, A. Pramanick and D. Viehland, Woodhead Publishing, 2021, pp. 43–84.
3 R. A. Kishore, in *Ferroelectric Materials for Energy Harvesting and Storage*, ed. D. Maurya, A. Pramanick and D. Viehland, Woodhead Publishing, 2021, pp. 85–106.
4 L. G. Hu, S. Dalgleish, M. M. Matsushita, H. Yoshikawa and K. Awaga, *Nat. Commun.*, 2014, **5**, 3279.
5 H. Y. Liu, H. Y. Zhang, X. G. Chen and R. G. Xiong, *J. Am. Chem. Soc.*, 2020, **142**, 15205–15218.
6 J. Sirohi, in *Ferroelectric Materials for Energy Harvesting and Storage*, ed. D. Maurya, A. Pramanick and D. Viehland, Woodhead Publishing, 2021, pp. 187–207.
7 P. Kumar, S. Singh, J. K. Juneja, C. Prakash and K. K. Raina, *Phys. B*, 2009, **404**, 1752–1756.
8 A. S. Tayi, A. Kaeser, M. Matsumoto, T. Aida and S. I. Stupp, *Nat. Chem.*, 2015, **7**, 281–294.
9 T. Akutagawa, T. Takeda and N. Hoshino, *Chem. Commun.*, 2021, **57**, 8378–8401.
10 Z.-X. Wang and W.-Q. Liao, *Science*, 2022, **375**, 1353–1354.
11 X. Chen, H. Qin, X. Qian, W. Zhu, B. Li, B. Zhang, W. Lu, R. Li, S. Zhang, L. Zhu, F. D. D. Santos, J. Bernholc and Q. M. Zhang, *Science*, 2022, **375**, 1418–1422.
12 S. Horiuchi, R. Kumai and Y. Tokura, *J. Am. Chem. Soc.*, 2005, **127**, 5010–5011.
13 S. Horiuchi, Y. Tokunaga, G. Giovannetti, S. Picozzi, H. Itoh, R. Shimano, R. Kumai and Y. Tokura, *Nature*, 2010, **463**, 789–792.
14 A. S. Tayi, A. K. Shveyd, A. C. Sue, J. M. Szarko, B. S. Rolczynski, D. Cao, T. J. Kennedy, A. A. Sarjeant, C. L. Stern, W. F. Paxton, W. Wu, S. K. Dey, A. C. Fahrenbach, J. R. Guest, H. Mohseni, L. X. Chen, K. L. Wang, J. F. Stoddart and S. I. Stupp, *Nature*, 2012, **488**, 485–489.
15 J. Harada, T. Shimojo, H. Oyamaguchi, H. Hasegawa, Y. Takahashi, K. Satomi, Y. Suzuki, J. Kawamata and T. Inabe, *Nat. Chem.*, 2016, **8**, 946–952.
16 H. Y. Ye, Y. Y. Tang, P. F. Li, W. Q. Liao, J. X. Gao, X. N. Hua, H. Cai, P. P. Shi, Y. M. You and R. G. Xiong, *Science*, 2018, **361**, 151–155.
17 C. R. Huang, Y. Li, Y. Xie, Y. Du, H. Peng, Y. L. Zeng, J. C. Liu and R. G. Xiong, *Angew. Chem., Int. Ed.*, 2021, **60**, 16668–16673.
18 Y. Ai, P. F. Li, M. J. Yang, Y. Q. Xu, M. Z. Li and R. G. Xiong, *Chem. Sci.*, 2022, **13**, 748–753.
19 M. Owczarek, K. A. Hujsak, D. P. Ferris, A. Prokofjevs, I. Majerz, P. Szklarz, H. Zhang, A. A. Sarjeant, C. L. Stern, R. Jakubas, S. Hong, V. P. Dravid and J. F. Stoddart, *Nat. Commun.*, 2016, **7**, 13108.

 This journal is © The Royal Society of Chemistry 2022

Published on 08 2022. Downloaded on 23/07/2024 8:47:18 .

20 M. Nespolo, *Acta Crystallogr., Sect. A: Found. Crystallogr.*, 2011, **67**, 561–563.
21 T. Schenk, E. Yurchuk, S. Mueller, U. Schroeder, S. Starschich, U. Böttger and T. Mikolajick, *Appl. Phys. Rev.*, 2014, **1**, 041103.
22 D. Damjanovic, in *The Science of Hysteresis*, ed. I. D. Mayergoyz, Academic Press, Oxford, 2006, pp. 337–465.
23 R. Sugano, Y. Hirai, T. Tashiro, T. Sekine, K. Fukuda, D. Kumaki, F. Domingues Dos Santos, A. Miyabo and S. Tokito, *Jpn. J. Appl. Phys.*, 2016, **55**, 10TA04.
24 P. P. Shi, Y. Y. Tang, P. F. Li, W. Q. Liao, Z. X. Wang, Q. Ye and R. G. Xiong, *Chem. Soc. Rev.*, 2016, **45**, 3811–3827.
25 M. E. Lines and A. M. Glass, *in Principles and Applications of Ferroelectrics and Related Materials*, Oxford University Press, Oxford, 2001.
26 M. T. O. Okenyi, L. E. Ratcliff and A. Walsh, *Phys. Chem. Chem. Phys.*, 2021, **23**, 2885–2890.
27 S. Ishihara, *J. Phys.: Condens. Matter*, 2014, **26**, 493201.
28 Z. Sun, T. Chen, J. Luo and M. Hong, *Angew. Chem., Int. Ed.*, 2012, **51**, 3871–3876.
29 S. Horiuchi and S. Ishibashi, *J. Phys. Soc. Jpn.*, 2020, **89**, 051009.
30 S. V. Kalinin, B. J. Rodriguez, S. Jesse, E. Karapetian, B. Mirman, E. A. Eliseev and A. N. Morozovska, *Annu. Rev. Mater. Res.*, 2007, **37**, 189–238.
31 L. F. Henrichs, J. Bennett and A. J. Bell, *Rev. Sci. Instrum.*, 2015, **86**, 083707.
32 H. Y. Zhang, X. G. Chen, Y. Y. Tang, W. Q. Liao, F. F. Di, X. Mu, H. Peng and R. G. Xiong, *Chem. Soc. Rev.*, 2021, **50**, 8248–8278.
33 M. E. Lines and A. M. Glass, *Principles and Applications of Ferroelectrics and Related Materials*, Oxford University Press, Oxford, 2001.
34 S. Horiuchi, F. Ishii, R. Kumai, Y. Okimoto, H. Tachibana, N. Nagaosa and Y. Tokura, *Nat. Mater.*, 2005, **4**, 163–166.
35 M. E. Lines and A. M. Glass, *Principles and Applications of Ferroelectrics and Related Materials*, Oxford University Press, Oxford, 2001.
36 B. Campbell, H. Stokes, D. Tanner and D. Hatch, ISODISPLACE computer programs, *J. Appl. Crystallogr.*, 2006, **39**, 607–614.
37 B. J. Campbell, J. S. Evans, F. Perselli and H. T. Stokes, *IUCr Comput. Comm. Newsl*, 2007, **8**, 81–95.
38 J. W. Lewis, J. L. Payne, I. R. Evans, H. T. Stokes, B. J. Campbell and J. S. O. Evans, *J. Am. Chem. Soc.*, 2016, **138**, 8031–8042.
39 A. Stroppa, P. Barone, P. Jain, J. M. Perez-Mato and S. Picozzi, *Adv. Mater.*, 2013, **25**, 2284–2290.
40 S. Kerman, B. J. Campbell, K. K. Satyavarapu, H. T. Stokes, F. Perselli and J. S. O. Evans, *Acta Crystallogr., Sect. A: Found. Crystallogr.*, 2012, **68**, 222–234.
41 H. Liu, W. Zhang, P. S. Halasyamani, H. T. Stokes, B. J. Campbell, J. S. O. Evans and I. R. Evans, *J. Am. Chem. Soc.*, 2018, **140**, 13441–13448.
42 H. Liu, M. J. Gutmann, H. T. Stokes, B. J. Campbell, I. R. Evans and J. S. O. Evans, *Chem. Mater.*, 2019, **31**, 4514–4523.
43 R. G. Kepler, *Annu. Rev. Phys. Chem.*, 1978, **29**, 497–518.
44 M. R. Srinivasan, *Bull. Mater. Sci.*, 1984, **6**, 317–325.
45 N. Sezer and M. Koç, *Nano Energy*, 2021, **80**, 105567.
46 C. R. Bowen, H. A. Kim, P. M. Weaver and S. Dunn, *Energy Environ. Sci.*, 2014, **7**, 25–44.
47 S. B. Lang, *Br. Ceram. Trans.*, 2004, **103**, 65–70.
48 N. A. Spaldin and M. Fiebig, *Science*, 2005, **309**, 391–392.
49 F. Kagawa, S. Horiuchi, M. Tokunaga, J. Fujioka and Y. Tokura, *Nat. Phys.*, 2010, **6**, 169–172.
50 J. Long, M. S. Ivanov, V. A. Khomchenko, E. Mamontova, J.-M. Thibaud, J. Rouquette, M. Beaudhuin, D. Granier, R. A. S. Ferreira, L. D. Carlos, B. Donnadieu, M. S. C. Henriques, J. A. Paixão, Y. Guari and J. Larionova, *Science*, 2020, **367**, 671–676.
51 A. Roy, R. Gupta and A. Garg, *Adv. Condens. Matter Phys.*, 2012, **2012**, 926290.
52 N. A. Spaldin, S. W. Cheong and R. Ramesh, *Phys. Today*, 2010, **63**, 38–43.
53 M. Fiebig, T. Lottermoser, D. Meier and M. Trassin, *Nat. Rev. Mater.*, 2016, **1**, 16046.
54 N. A. Hill, *J. Phys. Chem. B*, 2000, **104**, 6694–6709.
55 G. Giovannetti, S. Kumar, A. Stroppa, J. van den Brink and S. Picozzi, *Phys. Rev. Lett.*, 2009, **103**, 266401.
56 K. Kobayashi, S. Horiuchi, R. Kumai, F. Kagawa, Y. Murakami and Y. Tokura, *Phys. Rev. Lett.*, 2012, **108**, 237601.
57 S. Ishihara, *J. Phys. Soc. Jpn.*, 2010, **79**, 011010.
58 S. Ishihara, *J. Phys.: Condens. Matter*, 2014, **26**, 493201.
59 W. Q. Liao, Y. L. Zeng, Y. Y. Tang, H. Peng, J. C. Liu and R. G. Xiong, *J. Am. Chem. Soc.*, 2021, **143**, 21685–21693.
60 M. M. Yang and M. Alexe, *Adv. Mater.*, 2018, **30**, 1704908.
61 W. Q. Liao, B. B. Deng, Z. X. Wang, T. T. Cheng, Y. T. Hu, S. P. Cheng and R. G. Xiong, *Adv. Sci.*, 2021, **8**, 2102614.
62 Y. Y. Tang, J. C. Liu, Y. L. Zeng, H. Peng, X. Q. Huang, M. J. Yang and R. G. Xiong, *J. Am. Chem. Soc.*, 2021, **143**, 13816–13823.
63 Z. X. Wang, C. R. Huang, J. C. Liu, Y. L. Zeng and R. G. Xiong, *Chemistry*, 2021, **27**, 14831–14835.
64 W. J. Xu, K. Romanyuk, J. M. G. Martinho, Y. Zeng, X. W. Zhang, A. Ushakov, V. Shur, W. X. Zhang, X. M. Chen, A. Kholkin and J. Rocha, *J. Am. Chem. Soc.*, 2020, **142**, 16990–16998.
65 J. Park, D. Feng, S. Yuan and H. C. Zhou, *Angew. Chem., Int. Ed.*, 2015, **54**, 430–435.
66 F. Luo, C. B. Fan, M. B. Luo, X. L. Wu, Y. Zhu, S. Z. Pu, W. Y. Xu and G. C. Guo, *Angew. Chem., Int. Ed.*, 2014, **53**, 9298–9301.
67 D. E. Williams, J. A. Rietman, J. M. Maier, R. Tan, A. B. Greytak, M. D. Smith, J. A. Krause and N. B. Shustova, *J. Am. Chem. Soc.*, 2014, **136**, 11886–11889.
68 N. Sun, C. Wang, B. Yu, H. Wang, L. J. Barbour and J. Jiang, *ACS Appl. Mater. Interfaces*, 2022, **14**, 1519–1525.
69 B. Mondal, A. K. Ghosh and P. S. Mukherjee, *J. Org. Chem.*, 2017, **82**, 7783–7790.
70 M. Han, R. Michel, B. He, Y. S. Chen, D. Stalke, M. John and G. H. Clever, *Angew. Chem., Int. Ed.*, 2013, **52**, 1319–1323.

Published on 08 2022. Downloaded on 23/07/2024 8:47:18 .

71 M. Irie, T. Fukaminato, K. Matsuda and S. Kobatake, *Chem. Rev.*, 2014, **114**, 12174–12277.
72 D. Braga, *Angew. Chem., Int. Ed.*, 2012, **51**, 3516.
73 M. I. Mcmahon, R. J. Nelmes, W. F. Kuhs, R. Dorwarth, R. O. Piltz and Z. Tun, *Nature*, 1990, **348**, 317–319.
74 S. Horiuchi, R. Kumai and Y. Tokura, *Chem. Commun.*, 2007, 2321–2329.
75 R. Kumai, S. Horiuchi, H. Sagayama, T.-h Arima, M. Watanabe, Y. Noda and Y. Tokura, *J. Am. Chem. Soc.*, 2007, **129**, 12920–12921.
76 C. Shi, X. Zhang, C. H. Yu, Y. F. Yao and W. Zhang, *Nat. Commun.*, 2018, **9**, 481.
77 H. Sugimoto, *J. Phys.: Condens. Matter*, 1998, **10**, 1237–1246.
78 S. Koval, J. Kohanoff, R. L. Migoni and E. Tosatti, *Phys. Rev. Lett.*, 2002, **89**, 187602.
79 T. J. Negran, A. M. Glass, C. S. Brickenkamp, R. D. Rosenstein, R. K. Osterheld and R. Susott, *Ferroelectrics*, 2011, **6**, 179–182.
80 B. Batlogg, R. J. Cava, A. Jayaraman, R. B. van Dover, G. A. Kourouklis, S. Sunshine, D. W. Murphy, L. W. Rupp, H. S. Chen, A. White, K. T. Short, A. M. Mujsce and E. A. Rietman, *Phys. Rev. Lett.*, 1987, **58**, 2333–2336.
81 M. Itoh, R. Wang, Y. Inaguma, T. Yamaguchi, Y. J. Shan and T. Nakamura, *Phys. Rev. Lett.*, 1999, **82**, 3540–3543.
82 Y. Ai, H. P. Lv, Z. X. Wang, W. Q. Liao and R. G. Xiong, *Trends Chem.*, 2021, **3**, 1088–1099.
83 X. Mu, H. Y. Zhang, L. Xu, Y. Y. Xu, H. Peng, Y. Y. Tang and R. G. Xiong, *APL Mater.*, 2021, **9**, 051112.
84 Y. F. Xie, Y. Ai, Y. L. Zeng, W. H. He, X. Q. Huang, D. W. Fu, J. X. Gao, X. G. Chen and Y. Y. Tang, *J. Am. Chem. Soc.*, 2020, **142**, 12486–12492.
85 Y. Y. Tang, Y. Ai, W. Q. Liao, P. F. Li, Z. X. Wang and R. G. Xiong, *Adv. Mater.*, 2019, **31**, 1902163.
86 X. J. Song, T. Zhang, Z. X. Gu, Z. X. Zhang, D. W. Fu, X. G. Chen, H. Y. Zhang and R. G. Xiong, *J. Am. Chem. Soc.*, 2021, **143**, 5091–5098.
87 D. W. Fu, W. Zhang, H. L. Cai, Y. Zhang, J. Z. Ge, R. G. Xiong and S. D. Huang, *J. Am. Chem. Soc.*, 2011, **133**, 12780–12786.
88 P. F. Li, Y. Ai, Y. L. Zeng, J. C. Liu, Z. K. Xu and Z. X. Wang, *Chem. Sci.*, 2022, **13**, 657–664.
89 L. He, K. Xu, P.-P. Shi, Q. Ye and W. Zhang, *Adv. Electron. Mater.*, 2022, **8**(6), 2100635.
90 Y. Shimakawa, Y. Kubo, Y. Nakagawa, T. Kamiyama, H. Asano and F. Izumi, *Appl. Phys. Lett.*, 1999, **74**, 1904–1906.
91 A. von Hippel, R. G. Breckenridge, F. G. Chesley and L. Tisza, *Ind. Eng. Chem. Res.*, 1946, **38**, 1097–1109.
92 D. S. Jeong, R. Thomas, R. S. Katiyar, J. F. Scott, H. Kohlstedt, A. Petraru and C. S. Hwang, *Rep. Prog. Phys.*, 2012, **75**, 076502.
93 Z. Fan, J. Chen and J. Wang, *J. Adv. Dielectr.*, 2016, **06**, 1630003.
94 H. S. Choi, S. Li, I. H. Park, W. H. Liew, Z. Zhu, K. C. Kwon, L. Wang, I. H. Oh, S. Zheng, C. Su, Q. H. Xu, K. Yao, F. Pan and K. P. Loh, *Nat. Commun.*, 2022, **13**, 794.
95 Q. Pan, Z.-B. Liu, H.-Y. Zhang, W.-Y. Zhang, Y.-Y. Tang, Y.-M. You, P.-F. Li, W.-Q. Liao, P.-P. Shi, R.-W. Ma, R.-Y. Wei and R.-G. Xiong, *Adv. Mater.*, 2017, **29**, 1700831.
96 Y. F. Zhang, F. F. Di, P. F. Li and R. G. Xiong, *Chem. – Eur. J.*, 2022, **28**, e202102990.
97 J. Harada, *APL Mater.*, 2021, **9**, 020901.
98 J. Harada, N. Yoneyama, S. Yokokura, Y. Takahashi, A. Miura, N. Kitamura and T. Inabe, *J. Am. Chem. Soc.*, 2018, **140**, 346–354.
99 J. Harada, M. Takehisa, Y. Kawamura, H. Takahashi and Y. Takahashi, *Adv. Electron. Mater.*, 2022, **8**(6), 2101415.
100 J. Harada, Y. Kawamura, Y. Takahashi, Y. Uemura, T. Hasegawa, H. Taniguchi and K. Maruyama, *J. Am. Chem. Soc.*, 2019, **141**, 9349–9357.
101 J. Ichikawa, N. Hoshino, T. Takeda and T. Akutagawa, *J. Am. Chem. Soc.*, 2015, **137**, 13155–13160.
102 S. Horiuchi, R. Kumai and S. Ishibashi, *J. Mater. Chem. C*, 2021, **9**, 13739–13747.
103 T. Akutagawa, H. Koshinaka, D. Sato, S. Takeda, S. Noro, H. Takahashi, R. Kumai, Y. Tokura and T. Nakamura, *Nat. Mater.*, 2009, **8**, 342–347.
104 H. Cui, Z. Wang, K. Takahashi, Y. Okano, H. Kobayashi and A. Kobayashi, *J. Am. Chem. Soc.*, 2006, **128**, 15074–15075.
105 C. K. Yang, W. N. Chen, Y. T. Ding, J. Wang, Y. Rao, W. Q. Liao, Y. Xie, W. Zou and R. G. Xiong, *J. Am. Chem. Soc.*, 2019, **141**, 1781–1787.
106 P.-F. Li, Y.-Y. Tang, Z.-X. Wang, H.-Y. Ye, Y.-M. You and R.-G. Xiong, *Nat. Commun.*, 2016, **7**, 13635.
107 G. R. Desiraju, J. J. Vittal and A. Ramanan, *Crystal Engineering: A Textbook*, World Scientific Publishing Company, 2011.
108 R. B. Lin, Y. B. He, P. Li, H. L. Wang, W. Zhou and B. L. Chen, *Chem. Soc. Rev.*, 2019, **48**, 1362–1389.
109 S. Horiuchi, K. Kobayashi, R. Kumai and S. Ishibashi, *Nat. Commun.*, 2017, **8**, 14426.
110 S. Horiuchi, F. Kagawa, K. Hatahara, K. Kobayashi, R. Kumai, Y. Murakami and Y. Tokura, *Nat. Commun.*, 2012, **3**, 1308.
111 L. Noohinejad, S. Mondal, A. Wölfel, S. I. Ali, A. Schönleber and S. van Smaalen, *J. Chem. Crystallogr.*, 2014, **44**, 387–393.
112 K. Gotoh, T. Asaji and H. Ishida, *Acta Crystallogr., Sect. C: Struct, Chem.*, 2007, **63**, 17–20.
113 K. Saito, M. Amano, Y. Yamamura, T. Tojo and T. Atake, *J. Phys. Soc. Jpn.*, 2006, **75**, 033601.
114 S. Horiuchi, R. Kumai and Y. Tokura, *J. Mater. Chem.*, 2009, **19**, 4421–4434.
115 T. Asaji, J. Seliger, V. Žagar, M. Sekiguchi, J. Watanabe, K. Gotoh, H. Ishida, S. Vrtnik and J. Dolinšek, *J. Phys.: Condens. Matter*, 2007, **19**, 226203.
116 K. Lee, B. Kolb, T. Thonhauser, D. Vanderbilt and D. C. Langreth, *Phys. Rev. B*, 2012, **86**(10), 104102.
117 S. Horiuchi, R. Kumai, Y. Tokunaga and Y. Tokura, *J. Am. Chem. Soc.*, 2008, **130**, 13382–13391.
118 S. Horiuchi, R. Kumai and Y. Tokura, *J. Am. Chem. Soc.*, 2013, **135**, 4492–4500.

 This journal is © The Royal Society of Chemistry 2022

Published on 08 2022. Downloaded on 23/07/2024 8:47:18 .

119 S. Horiuchi, R. Kumai and Y. Tokura, *Adv. Mater.*, 2011, **23**, 2098–2103.
120 R. Kumai, S. Horiuchi, Y. Okimoto and Y. Tokura, *J. Chem. Phys.*, 2006, **125**, 084715.
121 E. Collet, M. H. Lemee-Cailleau, M. Buron-Le Cointe, H. Cailleau, M. Wulff, T. Luty, S. Y. Koshihara, M. Meyer, L. Toupet, P. Rabiller and S. Techert, *Science*, 2003, **300**, 612–615.
122 J. B. Torrance, J. E. Vazquez, J. J. Mayerle and V. Y. Lee, *Phys. Rev. Lett.*, 1981, **46**, 253–257.
123 J. B. Torrance, A. Girlando, J. J. Mayerle, J. I. Crowley, V. Y. Lee, P. Batail and S. J. LaPlaca, *Phys. Rev. Lett.*, 1981, **47**, 1747–1750.
124 A. Girlando, F. Marzola, C. Pecile and J. B. Torrance, *J. Chem. Phys.*, 1983, **79**, 1075–1085.
125 K. I. Shivakumar, K. Swathi, Goudappagouda, T. C. Das, A. Kumar, R. D. Makde, K. Vanka, K. S. Narayan, S. S. Babu and G. J. Sanjayan, *Chem. – Eur. J.*, 2017, **23**, 12630–12635.
126 A. K. Blackburn, A. C. Sue, A. K. Shveyd, D. Cao, A. Tayi, A. Narayanan, B. S. Rolczynski, J. M. Szarko, O. A. Bozdemir, R. Wakabayashi, J. A. Lehrman, B. Kahr, L. X. Chen, M. S. Nassar, S. I. Stupp and J. F. Stoddart, *J. Am. Chem. Soc.*, 2014, **136**, 17224–17235.
127 A. Narayanan, D. Cao, L. Frazer, A. S. Tayi, A. K. Blackburn, A. C. Sue, J. B. Ketterson, J. F. Stoddart and S. I. Stupp, *J. Am. Chem. Soc.*, 2017, **139**, 9186–9191.
128 D. Miyajima, F. Araoka, H. Takezoe, J. Kim, K. Kato, M. Takata and T. Aida, *Science*, 2012, **336**, 209–213.
129 K. Sato, Y. Itoh and T. Aida, *J. Am. Chem. Soc.*, 2011, **133**, 13767–13769.
130 U. D. Priyakumar and G. N. Sastry, *J. Org. Chem.*, 2001, **66**, 6523–6530.
131 S. Furukawa, J. Wu, M. Koyama, K. Hayashi, N. Hoshino, T. Takeda, Y. Suzuki, J. Kawamata, M. Saito and T. Akutagawa, *Nat. Commun.*, 2021, **12**, 768.
132 M. R. Katkova, S. S. Nosov, E. V. Chuprunov and E. L. Belokoneva, *Crystallogr. Rep.*, 2000, **45**, 647–649.
133 E. Kroumova, M. I. Aroyo and J. M. Perez-Mato, *Acta Crystallogr., Sect. B: Struct. Sci.*, 2002, **58**, 921–933.
134 S. Horiuchi, S. Ishibashi and Y. Tokura, in *Organic Ferroelectric Materials and Applications*, ed. K. Asadi, Woodhead Publishing, 2022, pp. 47–84.
135 Z. Zikmund, P. Vaněk, M. Havránková, B. Březina, M. člermák and M. Vásša, *Ferroelectrics*, 2011, **158**, 223–228.
136 R. D. King-Smith and D. Vanderbilt, *Phys. Rev. B: Condens. Matter Mater. Phys.*, 1993, **47**, 1651–1654.
137 Y. Noel, M. Catti and R. Dovesi, *Ferroelectrics*, 2004, **300**, 139–145.
138 Y. D. Huang, P. F. Hu, J. N. Song, Y. L. Li and A. Stroppa, *Chem. Phys. Lett.*, 2019, **730**, 367–371.
139 T. D. Cornelissen, M. Biler, I. Urbanaviciute, P. Norman, M. Linares and M. Kemerink, *Phys. Chem. Chem. Phys.*, 2019, **21**, 1375–1383.
140 S. Chen and X. C. Zeng, *J. Am. Chem. Soc.*, 2014, **136**, 6428–6436.
141 E. O. Pyzer-Knapp, L. Chen, G. M. Day and A. I. Cooper, *Sci. Adv.*, 2021, **7**, eabi4763.
142 G. M. Day and A. I. Cooper, *Adv. Mater.*, 2018, **30**, 1704944.
143 R. L. Greenaway and K. E. Jelfs, *Adv. Mater.*, 2021, **33**, 2004831.
144 R. L. Greenaway and K. E. Jelfs, *ChemPlusChem*, 2020, **85**, 1813–1823.
145 P. G. Boyd, A. Chidambaram, E. Garcia-Diez, C. P. Ireland, T. D. Daff, R. Bounds, A. Gladysiak, P. Schouwink, S. M. Moosavi, M. M. Maroto-Valer, J. A. Reimer, J. A. R. Navarro, T. K. Woo, S. Garcia, K. C. Stylianou and B. Smit, *Nature*, 2019, **576**, 253–256.
146 Y. Lin, M. Penna, C. D. Spicer, S. G. Higgins, A. Gelmi, N. Kim, S. T. Wang, J. P. Wojciechowski, E. T. Pashuck, I. Yarovsky and M. M. Stevens, *ACS Nano*, 2021, **15**, 4034–4044.
147 J. Valasek, *Phys. Rev.*, 1921, **17**, 475–481.